Evidence for atomic scale disorder in indium nitride from perturbed angular correlation spectroscopy

2005 J. Phys.: Condens. Matter 17 6037

(http://iopscience.iop.org/0953-8984/17/38/009)

INSTITUTE OF PHYSICS PUBLISHING JOURNAL OF PHYSICS: CONDENSED MATTER

J. Phys.: Condens. Matter **17** (2005) 6037–6046 doi:10.1088/0953-8984/17/38/009

Evidence for atomic scale disorder in indium nitride from perturbed angular correlation spectroscopy

R Dogra[1,2,6], S K Shrestha[3], A P Byrne[2,4], M C Ridgway[1], A V J Edge[3], R Vianden[5], J Penner[5] and H Timmers[3]

[1] Department of Electronic Materials Engineering, Research School of Physical Sciences and Engineering, Australian National University, ACT 0200, Australia
[2] Department of Nuclear Physics, Research School of Physical Sciences and Engineering, Australian National University, ACT 0200, Australia
[3] School of Physical, Environmental and Mathematical Sciences, University of New South Wales at the Australian Defence Force Academy, Canberra, ACT 2600, Australia
[4] Department of Physics, The Faculties, Australian National University, ACT 0200, Australia
[5] Helmholtz-Institut für Strahlen- und Kernphysik, Nussallee 14-16, 53115 Bonn, Germany

E-mail: rak109@rsphysse.anu.edu.au (R Dogra)

Received 8 June 2005, in final form 28 July 2005
Published 9 September 2005
Online at stacks.iop.org/JPhysCM/17/6037

Abstract

The crystal lattice of bulk grains and state-of-the-art films of indium nitride was investigated at the atomic scale with perturbed angular correlation spectroscopy using the ^{111}In/Cd radioisotope probe. The probe was introduced during sample synthesis, by diffusion and by ion implantation. The mean quadrupole interaction frequency $\nu_Q = 28$ MHz was observed at the indium probe site in all types of indium nitride samples with broad frequency distributions. The observed small, but non-zero, asymmetry parameter indicates broken symmetry around the probe atoms. Results have been compared with theoretical calculations based on the point charge model. The consistency of the experimental results and their independence of the preparation technique suggest that the origin of the broad frequency distribution is inherent to indium nitride, indicating a high degree of disorder at the atomic scale. Due to the low dissociation temperature of indium nitride, furnace and rapid thermal annealing at atmospheric pressure reduce the lattice disorder only marginally.

1. Introduction

In view of the technological success of gallium nitride and theoretical predictions of high peak electron mobility, indium nitride (InN) may be expected to play a prominent role in future device applications [1, 2]. This contrasts, however, with a lack of understanding of fundamental properties, illustrated by the debate about the electronic bandgap of InN, with

[6] On leave of absence from: College of Engineering and Technology, Gurdaspur-143521, India.

suggested values ranging from 0.7 to 1.9 eV [2]. Given a low value for the bandgap, the ternary alloy $In_xGa_{1-x}N$ might be employed in future optoelectronic devices which cover the visible spectrum of light from UV to red. The growth of high-quality InN is made difficult by its poor thermal stability. Some researchers have also cited [3] the large disparity of the atomic radii of In and N as a possible contributing factor to the difficulty in obtaining good quality InN.

InN remains the least understood of the important group III nitrides. Typically this material has high n-type background carrier concentrations resulting from native defects which may be due to nitrogen vacancies, nitrogen antisites or even the presence of unintentional impurities [1–3]. So far p-type doping has not been achieved. The presence of nitrogen vacancies would suggest that the material may be nitrogen poor, although this has recently been questioned on the basis of measurements with elastic recoil detection analysis, which have shown that state-of-the-art InN films tend to be nitrogen rich [4]. Using the positron annihilation technique, indium vacancies have, however, been observed in InN films [5].

In parallel to the development of high quality thin films, efforts are under way to synthesize nanometre-scale structures of InN, such as nanotubes [6]. It is hoped that such structures may allow the exploitation of quantum effects in optoelectronic devices based upon InN. While both wurtzite and zinc-blende lattices have been reported [1], the InN lattice is largely unexplored at the atomic scale. In principle such studies are possible with perturbed angular correlation (PAC) spectroscopy, which involves the introduction of radioisotope probes with concentrations of the order of ppm into the crystal lattice.

PAC spectroscopy [7] is based upon the interaction of the electric quadrupole moment of the probe atoms with the electric field gradient (EFG) of the material. The origin of the EFG can be either the non-cubic structure of a crystal lattice or the existence of defects in the immediate vicinity of the probe atoms. Using the PAC technique the EFG and its asymmetry parameter can be measured at the atomic scale. A value for the EFG at the indium site of the InN wurtzite lattice has been reported by Lorenz *et al* following measurements using the ^{111}In/Cd radioisotope probe [8]; however, the large magnitude is not consistent with the hexagonal wurtzite structure.

PAC spectroscopy offers a high degree of sensitivity to structural variations of the crystal lattice, since the EFG is mainly determined by the position and the charge of the atoms surrounding the probe atoms. This sensitivity is advantageous for studies of ion implantation and annealing, which are both important for semiconductor device processing. By ion-implanting the ^{111}In/Cd radioisotope probe into InN, the efficiency of reducing the implantation-associated lattice damage using varied annealing regimes can be sensitively studied using PAC spectroscopy, giving information which can guide future processing strategies.

In the present study PAC measurements of the EFG have been performed for indium sites in bulk grains of InN and for thin InN films grown with remote plasma enhanced chemical vapour deposition (RPECVD) and molecular beam epitaxy (MBE). The ^{111}In/Cd probe atoms were introduced in greatly differing ways including direct incorporation during sample synthesis, recoil implantation following nuclear fusion and low energy ion implantation as $^{111}In^+$ ions. Following implantation of the ^{111}In/Cd probe, furnace annealing and rapid thermal annealing of InN were performed under nitrogen atmosphere at atmospheric pressure and at temperatures reaching up to the dissociation temperature of the InN compound.

2. Experimental details

For PAC spectroscopy a material is doped with radioactive probe atoms which decay to a daughter isotope and populate an isomeric state of this isotope via γ-decay. Due to angular

momentum conservation, a second, correlated γ-ray emission, depopulating the isomeric state, is spatially anisotropic. The spatial anisotropy is changed by the interaction between the quadrupole moment of the probe nucleus in the isomeric state and the EFG associated with the crystal lattice. In particular, the interaction causes a modulation of the time-dependent angular correlation pattern of the emitted γ-rays, which reflects the EFG. The modulated time-dependent angular correlation pattern can be recorded as the perturbation function and interpreted. A detailed description of PAC spectroscopy can be found in [7].

In this work indium nitride was doped with the radioisotope probe ^{111}In/Cd using four different techniques. The first technique involved the direct incorporation of the probe atoms into polycrystalline bulk grains of InN. The latter were prepared from indium nitrate solution [9]. The $In(NO_3)_3$ was synthesized by dissolving a known quantity of pure indium metal (99.99%) in molar HNO_3. An activity of approximately 20–30 μCi of ^{111}In/Cd was added and the solution was slowly evaporated to yield indium nitrate crystals, which at elevated temperature (450 °C) thermally decomposed to yellow indium oxide powder. Finally, the indium oxide (In_2O_3) was loaded into a quartz boat and placed inside a tube furnace. Indium nitride was then synthesized over a period of 4 h by passing ammonia over the indium oxide at constant flow rate and at a temperature of 650 °C. The ammonia flow was maintained during cooling of the sample. The mass of the reaction product in the quartz boat was determined by weighing. Based on the initial amount of indium oxide, a 98% yield of indium nitride was inferred. The bulk grains were analysed by x-ray diffraction confirming the wurtzite lattice of InN.

Using the same procedure, polycrystalline bulk grains of InN were also synthesized without incorporating the ^{111}In/Cd probe. An activity of 20–30 μCi of the probe was then subsequently introduced via diffusion under vacuum at 500 °C for 24 h. This second doping technique led to the dissociation of some of the doped InN and the formation of In_2O_3, which, however, could be converted back to InN. This was achieved by placing the radioactive In_2O_3 sample inside a tube furnace and passing ammonia over it at constant flow rate and at a temperature of 650 °C for 4 h.

Applying a third technique, the ^{111}In/Cd probe was produced with the 14UD heavy-ion accelerator at the Australian National University via the nuclear fusion evaporation reaction ^{103}Rh(^{12}C, xpyn)^{111}Sn,^{111} Sb using a ^{12}C ion beam at an energy of 70 MeV. The reaction products ^{111}Sn and ^{111}Sb both decay to ^{111}In/Cd. In an appropriate experimental set-up, the recoil following the fusion reaction ion-implanted the probe atoms, with energies of up to 8 MeV, to a maximum depth of 3 μm into thin films of InN grown by MBE [10]. The implanted activity of ^{111}In/Cd was of the order of 1–2 μCi.

The fourth technique also employed ion implantation as a way of introducing the ^{111}In/Cd probe into InN samples. Another sample of the same MBE-grown film, which was recoil implanted with the probe, and an InN film grown by RPECVD were implanted with 160 keV $^{111}In^+$ ions using the radioisotope implanter at the Helmholtz-Institut für Strahlen-und Kernphysik in Bonn. Implanted activities were of the order of 5 μCi.

All ion-implanted samples were studied with PAC spectroscopy as implanted and following several annealing steps at increasing temperatures. The recoil-implanted InN films were annealed under nitrogen in a quartz tube furnace for 30 min, whereas the film implanted with $^{111}In^+$ ions underwent rapid thermal annealing for 2 min.

PAC measurements were performed utilizing the hyperfine interaction of the 245 keV, $5/2^+$ spin state of ^{111}Cd. Twelve delayed coincidence spectra were simultaneously recorded at room temperature using a standard PAC set-up with four BaF_2 detectors arranged in planar 90°–180° geometry. The detector system has a time resolution of ∼500 ps. The time-dependent perturbation functions $R(t)$ have been generated from the background subtracted coincidence

counts $C(\theta, t)$ according to

$$R(t) = 2\left[\frac{C(180^\circ, t) - C(90^\circ, t)}{C(180^\circ, t) + 2C(90^\circ, t)}\right] \tag{1}$$

where the $C(\theta, t)$ are the geometric mean-values of the number of coincidences in spectra recorded at angle θ. The functions $R(t)$ have been fitted using a model for the static nuclear-electric-quadrupole interaction which leads to

$$R(t) = A_{22}G_{22}(t) = A_{22}\sum_i f_i G^i_{22}(t) \tag{2}$$

where A_{22} is the unperturbed angular correlation coefficient, f_i are the fractional site populations and $G^i_{22}(t)$ are the corresponding perturbation factors given by

$$G_{22}(t) = \sum_{n=0}^{3} S_{2ni}(\eta_i)\cos(\omega_{ni}(\eta_i)t)\exp\left(\frac{-(\delta_i\omega_{ni}t)^2}{2}\right)\exp\left(\frac{-(\tau_R\omega_{ni}t)^2}{2}\right). \tag{3}$$

Here the primary frequencies ω_n and their amplitudes S_{2n} are related to the hyperfine splitting of the intermediate nuclear level and depend on the nuclear quadrupole frequency $\omega_Q = eQV_{zz}/4I(2I-1)\hbar$ and the asymmetry parameter $\eta = (V_{xx} - V_{yy})/V_{zz}$, where V_{xx}, V_{yy} and V_{zz} are the elements of the EFG tensor in its principal axis system. As usual, V_{zz} is the largest component of the EFG tensor and generally only the spin independent quadrupole interaction frequency defined by $\nu_Q = eQV_{zz}/h$ is used, where Q is the nuclear electric quadrupole moment of the intermediate level. The known quadrupole moment of 0.83 b for the $I^\pi = 5/2^+$ intermediate level of ^{111}Cd has been used to determine V_{zz}. Effects due to the finite time-resolution τ_R of the detectors and the finite width δ of the EFG distribution are included in equation (3). For all samples investigated here, the amplitudes S_{2n} in equation (3) have been fixed to the random powder values to fit experimental data.

3. Results

X-ray diffraction confirmed that all InN samples have wurtzite structure and no contaminating phases. For the films investigated scanning electron microscopy showed columnar structures of InN grains oriented along the ⟨0001⟩ axis and assured state-of-the-art growth quality.

Figure 1 displays the perturbation functions $R(t)$ measured with PAC spectroscopy for the polycrystalline bulk grains of InN. The fits to the experimental data are based upon the theoretical function given as equation (3). In general, the frequencies of oscillations in $R(t)$ are proportional to the strengths of the EFGs observed. The corresponding amplitudes give the fraction of the ^{111}In/Cd probe atoms exposed to a particular EFG. Damping of an oscillation indicates that the EFG is not single valued, but that a distribution of EFGs exists. The severity of the damping is related to the finite width of this EFG distribution.

The experimental data in figure 1(a) for bulk grains into which the ^{111}In/Cd probe was incorporated during synthesis show the onset of a strongly damped low frequency oscillation for $R(t)$. Fitting reveals the existence of a broad distribution of EFGs which is centred at the interaction frequency $\nu_{Q1} = 28$ MHz. The asymmetry parameter is $\eta \sim 0.3$. In an attempt to investigate if the origin of the broad width of the EFG distribution is related to mobile point defects, PAC spectroscopy was also performed on the same sample at liquid nitrogen temperature where such defects are less mobile. Figure 1(b) shows the function $R(t)$ from this measurement, which is unchanged, suggesting the absence of a dynamical effect due to mobile point defects. In electron capture decay of ^{100}Pd to ^{100}Rh, the holes produced within 1 ns may distort the electronic surroundings of the probe nuclei, which may result in a damping of the

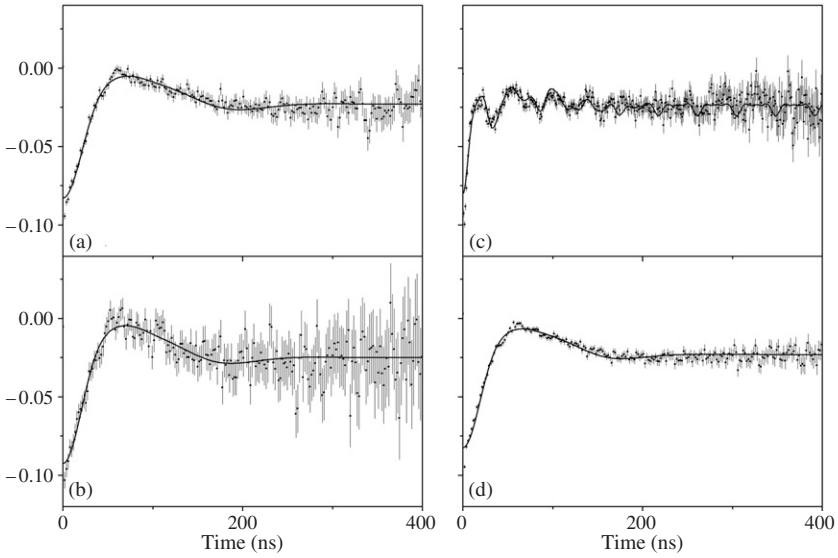

Figure 1. The measured perturbation functions $R(t)$ from PAC spectroscopy of InN bulk grains with the ^{111}In/Cd probe. (a) Probe introduced during InN synthesis and spectroscopy at room temperature. (b) The same sample measured at liquid nitrogen temperature. (c) Probe introduced via diffusion and spectroscopy at room temperature showing signatures of In_2O_3 contamination. (d) Re-measurement of the same sample following sintering which converted the In_2O_3 to InN. The fits are based on equation (3).

PAC spectrum, known as after-effects. We rule out the possibility of dynamic broadening due to after-effects because of the lack of a significant difference in PAC spectra measured at the different temperatures. A slightly larger anisotropy is observed at liquid nitrogen temperature in comparison to room temperature measurement due to the large sample–detector distance.

The perturbation functions $R(t)$ measured on bulk grains into which the ^{111}In/Cd had been introduced by diffusion are in figure 1(c). Three interaction frequencies are observed and can be fitted. The fit includes a slow interaction frequency $\nu_{Q1} = 28$ MHz with $\eta \sim 0.3$, as in figures 1(a) and (b), and two high frequencies $\nu_{Q2} = 119$ MHz with $\eta = 0.7$ and $\nu_{Q3} = 153.6$ MHz with $\eta = 0$. The latter two frequencies correspond to In_2O_3 which formed during the diffusion of the ^{111}In/Cd probe. Oxidation of InN has indeed been observed by others even under high vacuum at a temperature of 550 °C [11]. Sintering in a tube furnace at 650 °C in the presence of flowing ammonia, however, converted the In_2O_3 back to InN. The function $R(t)$ measured after sintering can be seen in figure 1(d). The high frequencies are absent and the data can be fitted with ν_{Q1} and a broad EFG distribution similar to the results in figures 1(a) and (b).

The results shown in figure 1 identify $\nu_{Q1} = 28$ MHz as the correct interaction frequency for ^{111}In/Cd probe atoms at the indium site of the wurtzite InN lattice. The observed value is supported by the following argument. Since the hexagonal wurtzite and the zinc-blende lattice are quite similar in terms of their nearest neighbours, one should expect vanishingly small EFGs at cation/anion sites in both lattices [12][7]. The measured frequency $\nu_{Q1} = 28$ MHz for the indium site in InN corresponds to an EFG of 1.43×10^{21} V m^{-2} which is of the same order as the EFGs observed at the Al site in AlN (0.61×10^{21} V m^{-2}) [13] and the Ga site

[7] Probes different than host cations/anions, because of charge difference, radii difference etc, generally modify the charge distribution in the lattice and give strong EFGs.

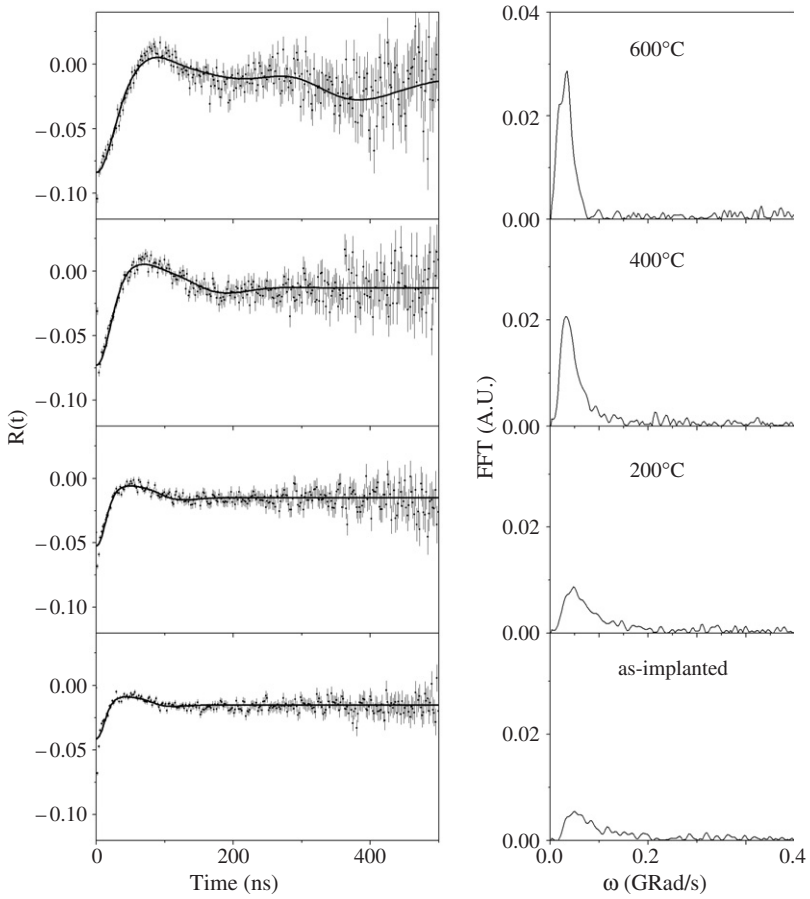

Figure 2. On the left the measured perturbation functions $R(t)$ and fits and on the right the respective Fourier transforms for a MBE-grown InN film which was recoil implanted with the ^{111}In/Cd probe. PAC spectroscopy was performed on the as-implanted sample at room temperature and after furnace annealing at the indicated temperatures.

in GaN (0.705×10^{21} V m^{-2}) [14]. The observation of a high interaction frequency in an earlier PAC study of InN [8] with the same radioisotope probe can thus be attributed to In_2O_3 contamination.

The least squares fitted functions $R(t)$, and their respective Fourier transforms, measured at room temperature for the MBE-grown InN sample, are shown in figure 2. The measurements were carried out on the as-implanted film and after subsequent furnace annealing at temperatures of 200, 400, and 600 °C. The strong damping of $R(t)$ for the as-implanted sample indicates that the probe atoms are exposed to a broad distribution of EFGs. The Fourier transform also reflects the broad distribution of interaction frequencies. The environment of the as-implanted ^{111}In/Cd probe atoms in the InN lattice is characterized by an average value of the interaction frequency of $\nu_Q = 49.0$ MHz with an associated distribution width of approximately $\Delta\nu_Q = 16.0$ MHz. Accordingly, the majority of the probe atoms are incorporated in highly disordered, non-unique lattice environments.

As visible in figure 2, furnace annealing reduces the damping somewhat and lowers the interaction frequency. After annealing at 400 °C the width of the EFG distribution is, however,

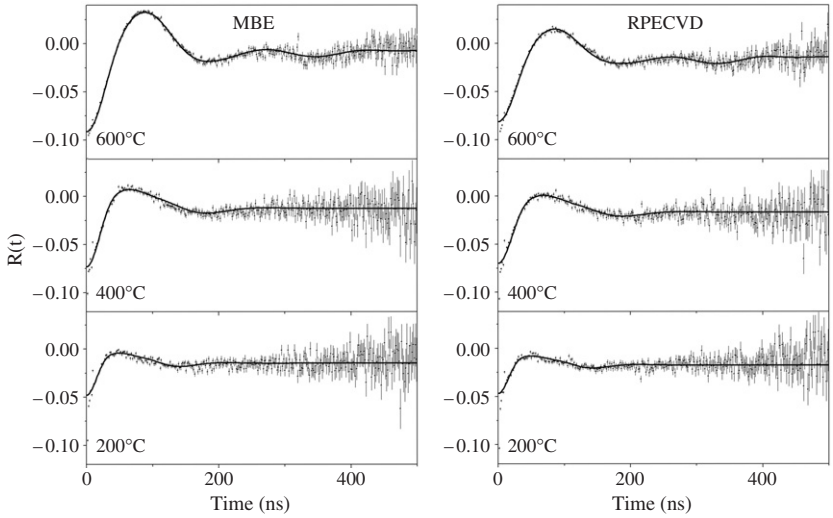

Figure 3. On the left the measured and fitted perturbation functions $R(t)$ for the same MBE film as in figure 2, however with the ^{111}In/Cd probe introduced by implantation of 160 keV $^{111}In^{+}$ ions. On the right the same for an InN film grown by RPECVD. The PAC spectroscopy was carried out after rapid thermal annealing at the temperatures indicated.

essentially unchanged, while the interaction frequency is reduced to $\nu_Q = 28.7$ MHz, the value expected for the indium site in InN. The asymmetry parameter is $\eta \sim 0.3$. Following furnace annealing at 600 °C indium droplets could be observed on the surface of the film and the function $R(t)$ shows an additional low interaction frequency of 17 MHz originating from probe atoms in indium metal.

The results for the MBE-grown film reflect those obtained for InN bulk grains. Furnace annealing within the temperature range accessible at atmospheric pressure is not sufficient to significantly reduce the lattice disorder. In an effort to investigate if the observed lattice disorder is mainly inflicted during the recoil-implantation of the ^{111}In/Cd probe, a second sample of the MBE-grown film was also prepared by implanting the probe as 160 keV $^{111}In^{+}$ ions. Using the same implantation parameters the probe was also introduced into an InN film grown by RPECVD. The results of the PAC spectroscopy performed on these two samples are shown in figure 3.

Following implantation for both samples broad frequency distributions have been observed, which are analogous to those obtained for the bulk grains and the recoil-implanted MBE-grown film. The function $R(t)$ measured after rapid thermal annealing at 400 °C is also very similar to that observed after furnace annealing of the recoil-implanted film. Interestingly, no significant difference exists between the film from MBE growth and that grown by RPECVD. It appears that the disorder is neither the result of a particular growth technique nor dependent on the technique of probe introduction, but a feature of the InN lattice at the atomic scale.

Further rapid thermal annealing in nitrogen atmosphere at 600 °C did not significantly alter either the frequency distribution for the MBE-grown film, or that for the film from RPECVD growth. The fits, however, reveal less damping and a slight reduction of the interaction frequency to 21.0 MHz, with an increased asymmetry parameter of $\eta \sim 0.6$. Importantly, and in contrast to the film prepared by recoil implantation, there is no signature of any ^{111}In/Cd probe atoms with indium metal environment. Instead an additional low interaction frequency, different from that for indium metal, is observed for a small probe fraction (5–7%) with values

of 19.4 MHz for the MBE-grown film and 20.3 MHz for the RPECVD film, respectively. The origin of this frequency may, nevertheless, be related to the onset of dissociation in the InN lattice, which nominally occurs above 550 °C. The appearance of indium droplets on annealing at 600 °C on the recoil-implanted MBE sample may be due to the longer furnace annealing time, leading to partial dissociation of the InN lattice.

4. Discussion

The measured quadrupole interaction frequency ($\nu_Q = 28$ MHz) at indium sites in InN for the radioisotope probe ^{111}In/Cd is consistent with the results of earlier PAC and NMR studies of other wurtzite compounds including AlN and GaN. The observed weak EFG, giving rise to this low interaction frequency, corresponds to the substitutional incorporation of probe atoms at the cation site. The broad distribution of EFGs observed with PAC spectroscopy for InN indicates the existence of a diverse set of point defects and other disorder in the immediate atomic neighbourhood of the cation. One important defect type is the indium vacancy identified most recently by positron annihilation spectroscopy in MBE-grown InN with vacancy concentrations of the order of 10^{16-18} cm^{-3}. At such concentrations this defect can be expected to significantly broaden the EFG distribution. The observed weak EFG at the indium site is consistent with the indium vacancies as the presence of near-neighbour nitrogen vacancies would lead to a strong EFG. The small, but non-zero value of asymmetry parameter ($\eta \sim 0.3$) in the wurtzite phase indicates the distortion of the InN lattice in the vicinity of the ^{111}In/Cd probe atoms. The observed broken symmetry may possibly be due to the presence of distant defects in the crystal lattice. This kind of behaviour has been simulated by Forker for random distributions of static crystal defects leading to broad EFG distributions and an increased asymmetry parameter [15].

The point charge model (PCM) offers an insight into the behaviour of many ionic crystals and also some insulators. The valence band charge density calculations based upon the pseudo-potential method have shown about 60% ionic character in the InN crystal lattice [16]. Therefore, it is appropriate to consider the closed shell electronic configuration for In^{3+} ([Kr] $4d^{10}$) and N^{3-} ($1s^2 2s^2 2p^6$) ions. Assuming a dominant contribution from lattice ions and neglecting the electronic contribution of valence electrons, the PCM may thus be successfully applied to calculate EFG parameters in the InN lattice. PCM calculations have been performed, calculating V_{zz} and η for cation (indium) sites in the InN lattice with the lattice sum given by

$$V_{zz}^{\text{latt}} = \sum_k Z_k \frac{3x_{ki}x_{kj} - \delta_{ij} r_k^2}{r_k^5}. \tag{4}$$

In the above expression, Z_k denotes the ionic charge, x_{ki} and x_{kj} are the coordinates and r_k is the distance of the kth ion from the site where the EFG is calculated, located at the origin of the coordinated system for simplicity. Formal charges of +3 and −3 (fully ionized states) were assigned to cations and anions, respectively. The lattice sum was performed numerically to within a sphere of radius 200 Å with the probe at the origin. The lattice sum converged very slowly. The lattice parameters and the atomic positions were taken from Rietveld analysis [17, 18]. In order to compare with the experimental values, the contribution originating from the core deformation of the probe under the presence of the lattice EFG has to be added. This contribution can be computed using the Sternheimer anti-shielding factor γ_∞ of the probe atom. It is given by $\gamma_\infty V_{zz}^{\text{latt}}$. The sum of this contribution and V_{zz}^{latt} is called the 'ionic contribution', and the EFG can be written as $V_{zz}^{\text{PCM}} = (1 - \gamma_\infty) V_{zz}^{\text{latt}}$.

The results of the PCM calculation for V_{zz} and η are summarized in table 1 for the important III nitride compounds. Experimental results are included in this table for comparison. While

Table 1. Experimentally determined room temperature values of η and V_{zz} for AlN, GaN and InN, respectively, compared with those calculated using the point charge model (PCM) for hexagonal wurtzite crystal structures. γ_∞ represents the Sternheimer anti-shielding factor.

Sample	Lattice parameter (Å)	Exp. Method	Probe atoms at cation sites	η	V_{zz} ($\times 10^{21}$ V m^{-2})	η^{PCM}	$\lvert V_{zz}^{\mathrm{PCM}}\rvert$ ($\times 10^{21}$ V m^{-2})	Remarks
AlN	$a = 3.1119$ $c = 4.9809$ $u = 0.3869$	NMR	Al ($\gamma_\infty = -3.3$)	0.0	0.610	0.0	0.638	Ref. [13] This work
GaN	$a = 3.2894$ $c = 5.1861$ $u = 0.3789$	NMR	Ga ($\gamma_\infty = -9.5$)	0.0	0.705	0.0	0.370	Ref. [14] This work
InN	$a = 3.5377$ $c = 5.7037$ $u = 0.3769$	PAC	In ($\gamma_\infty = -29.27$)	03	1.43	0.0	0.266	This work

the agreement between the experimental and calculated values of the asymmetry parameter η is reasonably good for all compounds, the agreement between theory and experiment for V_{zz} in InN is rather poor. The EFG is strongly influenced by the u-parameter which has a relatively large uncertainty for InN. The u-parameter describes the relative length of the cation–anion bond aligned along the c-axis of the lattice. A small change in u-parameter drastically changes the EFG. Since the PAC spectroscopy has shown that the InN crystal lattice has a large number of different types of defects, significant variation of the u-parameter within the lattice may be expected. The disagreement between experimental and calculated EFG values may also be due to the covalent contribution to the EFG that has not been accounted for in the point charge model calculations. Recently, first-principle calculations based upon full-potential linearized augmented plane wave (FP-LAPW) [19] have been applied successfully to reproduce the experimental results. Thus, such electronic structure calculations may also be required to describe correctly the effects of covalent bonding in nitride semiconductors.

5. Conclusions

The measured interaction frequency of 28 MHz at the indium probe site in an InN lattice is an important benchmark result enabling further, detailed PAC spectroscopy of the atomic-scale lattice structure of this material. In particular, the effects of ion implantation and annealing on future high-quality InN films may be studied. At room temperature the mean electric field gradient at the cation site in InN has been determined as $V_{zz} = 1.43 \times 10^{21}$ V m^{-2}. This is consistent with measurements for other III nitrides. Calculations of V_{zz} and the asymmetry parameter η for the cation site of AlN, GaN and InN using the point charge model give reasonable agreement, although the V_{zz}-value is somewhat underestimated for InN.

The observation of a small, but non-zero, value of the asymmetry parameter indicates broken symmetry in the InN lattice around the cation site. This is likely due to lattice deformation produced by distant defects. A diverse set of many different defects, leading to atomic-scale lattice disorder, causes a significant broadening of the electric field gradient distribution. This evidence, which is consistent with a large fraction of indium vacancies in InN, appears independent of the introduction of the radioisotope probe into the lattice. At the atomic scale, state-of-the-art InN films from MBE and RPECVD growth show a high degree of local disorder similar to what is observed for bulk grains of InN. This suggests that the defects are inherent to the lattice of InN and may limit the synthesis of nanometre-scale structures of

InN. Both furnace and rapid thermal annealing at atmospheric pressure have been shown to only marginally reduce the InN lattice disorder within the accessible temperature range.

Acknowledgments

The authors wish to thank the academic and accelerator staff of the ANU heavy-ion facility for their support during this work. APB and MCR thank the Australian Research Council for financial support.

References

[1] Bhuiyan A G, Hashimoto A and Yamamoto A 2003 *J. Appl. Phys.* **94** 2779 and references therein
[2] Butcher K S A 2004 *Adv. Mater. Electron.* 1
[3] Strike R and Morkoc H 1992 *J. Vac. Sci. Technol.* B **10** 1237
[4] Shrestha S K, Timmers H, Scott Butcher K S A, Wintrebert-Fouquet M and Chen P P-T 2005 *Nucl. Instrum. Methods Phys. Res.* B **234** 291
[5] Laakso A, Oila J, Kemppinen A, Saarinen K, Egger W, Liszkay L, Sperr P, Lu H and Schaff W J 2004 *J. Cryst. Growth* **269** 41
[6] Schwenzer B, Loeffler L, Seshadri R, Keller S, Lange F F, DenBaars S P and Mishra U K 2004 *J. Mater. Chem.* **14** 637 and references therein
[7] Frauenfelder H and Steffen R M 1968 *Alpha, Beta and Gamma Ray Spectroscopy* ed K Siegbahn (Amsterdam: North-Holland) p 997
Forkel-Wirth D 1999 *Rep. Prog. Phys.* **62** 527
Wichert Th and Deicher M 2001 *Nucl. Phys.* A **693** 327
[8] Lorenz K, Vianden R, Pearton S J, Abernathy C R and Zavada J M 2000 *MRS Internet J. Nitride Semicond. Res.* **5** 1
[9] Murali A K, Barve A D and Risbud S H 2002 *Mater. Sci. Eng.* B **96** 111
[10] Bezakova E, Byrne A P, Glover C J, Ridgway M C and Vianden R 1999 *Appl. Phys. Lett.* **75** 1923
[11] Hura T-B, Leeb I J, Parkc H L, Hwanga Y-H and Kim H-K 2004 *Solid State Commun.* **130** 397
[12] Dietrich M, Kortus J, Cordts W and Unterricker S 1998 *Phys. Status Solidi* b **207** 13
[13] Han O H, Timken H K C and Oldfield E 1988 *J. Chem. Phys.* **89** 6046
[14] Denninger G and Reiser D 1997 *Phys. Rev.* B **55** 5073
[15] Forker M 1973 *Nucl. Instrum. Methods* **106** 121
[16] Tadjer A, Abbar B, Rezki M, Dufour J P, Aourag H and Certier M 2000 *Mater. Chem. Phys.* **62** 75
[17] Paszkowicza W, Cerny R and Krukowski S 2003 *Powder Diffr.* **18** 114
[18] Paszkowicz W, Podsiado S and Minikayev R 2004 *J. Alloys Compounds* **382** 100
[19] Blaha P, Dufeck P, Schwarz K and Haas H 1996 *Hyperfine Interact.* **97/98** 3 and references therein